Title
LIQUID-SOLID TRANSFORMATION KINETICS IN Al2O3

Authors
Das, Amio R.
Fulrath, Richard M.

Publication Date
1963-12-26

UCRL-11166

University of California
Ernest O. Lawrence
Radiation Laboratory

LIQUID-SOLID TRANSFORMATION KINETICS IN Al_2O_3

Berkeley, California

DISCLAIMER

For publication in Proceedings of the
5th International Symposium on the Reactivity of
Solids - Munich, Germany, Spring 1964

UCRL-11166

UNIVERSITY OF CALIFORNIA

Lawrence Radiation Laboratory
Berkeley 4, California

AEC Contract No. W-7405-eng-48

LIQUID-SOLID TRANSFORMATION KINETICS IN Al_2O_3

Amio R. Das and Richard M. Fulrath

December 26, 1963

ABSTRACT

A D.C. arc plasma torch was used to subject sized particles of synthetic sapphire in the range of 9 to 104 microns to rapid melting and resolidification. In order to study the formation of metastable phases of alumina, the size and apparent density of spheroidized particles were used as parameters in determining quenching rates. A hypothesis based on the kinetics of nucleation of the crystalline solid phases from the supercooled liquid droplets is proposed to explain the ratio of the metastable phases to the stable α phase. Experimental data relating this ratio with quench rates of the liquid droplets are presented.

UCRL-11166

LIQUID-SOLID TRANSFORMATION KINETICS IN Al_2O_3

Amio R. Das and Richard M. Fulrath

Department of Mineral Technology and
Inorganic Materials Research Division
Lawrence Radiation Laboratory
University of California, Berkeley, California

INTRODUCTION

Aluminum oxide has been spheroidized in both oxygen-hydrogen torches[1] and in D.C. arc plasma jets.[2] Flame spraying of alumina coatings on both a commercial and laboratory scale have also used these two devices.[2, 3] During these processes both stable α alumina and metastable phases of alumina have been formed.

Alumina has one stable phase (α) between room temperature and its melting point.[4] X-ray diffraction studies to 2000 °C have not shown the existence of a high temperature modification.[5] Various metastable phases of near anhydrous or anhydrous alumina (γ, δ, θ, κ, χ and η) have been identified.[4, 6, 7] Most of these phases are formed by the decomposition of various alumina salts such as hydrates, sulphates, nitrates, etc. In the absence of stabilizing impurities the metastable phases are all converted to α Al_2O_3 at approximately 1200 °C. When α Al_2O_3 is heated above 2000 °C it has been reported that a highly defect structure is formed.[8] This has been interpreted to be the result of structural breakdown near the melting point as has been observed in a number of crystalline solids[9a] and not as the formation of a new phase.

Plummer[1] in spheroidization studies using an oxygen-hydrogen flame hypothesized that metastable solid phases would be formed from the liquid due to the greater mobility of aluminum ions relative to the oxygen ions in the crystal and the possible decreased coordination number of aluminum ions in the liquid. Therefore, a crystalline solid is formed representative of the

geometric substructures in the liquid.

In this investigation the kinetics of nucleation of metastable phases and stable α alumina is suggested as being the controlling factor in determining the crystalline phase present at room temperature after the quenching of a liquid droplet.

THEORY

Steady State Nucleation

The free energy relationships between a liquid and two solid phases can be diagrammatically illustrated as shown in Figure 1. The lowest free energy will determine the stable phase at any temperature, T. If one solid phase, A, has its free energy related to that of the liquid as shown then the other solid phase, B, may appear as a stable phase at high temperatures or be at all times unstable relative to A. These two conditions are illustrated by the two dashed curves. In the case where B is stable at high temperatures the transformation temperature (A→B) will occur. In the case when B is unstable relative to A then a pseudo melting temperature of B will be evident as shown (T_{m_b}).

In the case of alumina where the alpha phase is reported stable to the melting point then, the metastable phases of interest in this study (γ and δ) would have pseudo melting temperatures lower than that of the α phase and the free energy relationships would be as shown by the upper dashed curve in Figure 1.

Classical theory of homogeneous nucleation as developed by Volmer, Becker, and Doring [10] and applied to the liquid-solid transition gives the steady state nucleation rate as;

$$I = \frac{nn^* kT}{h} \exp\left[\frac{-16\,\pi\sigma^3 T_m^2}{3kT\,(T_m - T)^2\,\Delta H_f^2} - \frac{E_n}{kT}\right] \qquad (1)$$

where:

I = number of nucleii appearing per cm^3 per sec.

n = number of molecules per unit volume of liquid.

n^* = number of molecules required to form a stable nucleus.

σ = solid-liquid interface energy in ergs per cm^2.

ΔH_f = volumetric heat of fusion in ergs per cm^3.

k = Boltzmann constant.

h = Planck's constant.

T_m = equilibrium melting temperature.

T = actual liquid temperature.

E_n = activation energy for diffusion in the liquid which for convenience may be taken as the activation energy for viscosity in liquid alumina. (11)

$(T_m - T)$ = degree of super cooling.

If there exists the possibilty of nucleation of two different solid phases (α, the stable species, and m, a metastable species) which have different constants σ, T_m and ΔH_f in equation 1 then the nucleation rate vs. temperature relationship between these two phases may be as shown in Figure 2. The metastable phase may have a nucleation rate as shown by I_m' which is always lower than I_α or if I_m crosses I_α as shown then at temperatures above T_c the nucleation of α is favored and below T_c the nucleation of m is favored. In any case the ratio of the nucleation rates of α and m, R_n, at any temperature, T, is:

$$R_n(T) = \frac{I_m}{I_\alpha} \qquad (2)$$

Nonsteady State Nucleation

If in a system such as those encountered when small crystal particles are liquefied and quenched, and the crystal growth rate is so rapid that a nucleus once formed determines the crystalline modification of the solidified liquid

droplet then the ratio of the number of spheres appearing as the metastable phase to the number of spheres appearing as the stable phase, $R_p = R_n$ provided that nucleation occurs at a temperature, T, which is below T_{m_m}.

The D.C. plasma jet [12] when used to melt and spheroidize a crystalline feed imposes dynamic conditions such that the exact time-temperature history is impossible to determine. Also, equation 1 is for steady state conditions describing the nucleation of a solid crystalline phase from a liquid. [9b] The time to attain steady state nucleation is determined by the fluidity of the liquid as shown by Hillig. [13] Similar calculations as those described by Hillig were made using an estimated viscosity for liquid alumina. [11] The results of such calculations indicate that the steady state nucleation rate should be attained in less than one microsecond. However, based on particle velocity measurements it is estimated that particles are subjected to a heating and cooling cycle of approximately milliseconds duration. Therefore, equation 1 can be used provided that the temperature, T, be replaced by an estimated function of time T(t), based on the calculated heat transfer characteristics of a liquid droplet.

With the assumption that a drop of liquid of volume v is cooled in such a manner that as soon as n nucleii of solid appear they grow at a sufficient rate, G_v, so that the drop is totally converted to the solid before any more nucleii appear. Then:

$$n = \frac{v}{G_v \tau} \geq 1 \qquad (3)$$

where:

v = volume of the liquid drop in cm^3.

G_v = volumetric growth rate per nucleus in cm^3 per sec.

τ = a small but finite time interval.

Let N, the number of liquid droplets at time t, equal $N_o F(t)$ where N_o is the original number of liquid droplets and F(t) is a function of time such that $F(0) = 1$ and $F(\infty) = 0$. In a small interval of time, dt, about t, the volume

of liquid drops disappearing by solidification is equal to the rate of solidification times the time interval, dt. or,

$$-dN = I(t)\, N(t)\, \frac{v}{n}\, dt = ING_v \tau\, dt \tag{4}$$

and

$$-\frac{dN}{dt} = ING_v \tau = IN\, \frac{v}{n} \tag{5}$$

For a liquid that has a relatively constant value of the volumetric growth rate, the value of v/n in equation 5 will be essentially constant. This assumption should be applicable for low viscosity liquids where the growth rate of the solid phase is not strongly dependent on the diffusivity in the liquid and levels out with decreasing temperature.

From equation 5 and $N = N_o\, F(t)$ then the rate of solidification is:

$$I\, N\, \frac{v}{n} = I\, N_o\, \frac{v}{n}\, F(t) = -N_o\, F'(t) \tag{6}$$

and

$$F = \exp\left[-\frac{v}{n} \int_o^t I(z)\, dz\right] \tag{7}$$

If both a stable species, α, and a metastable species, m, can nucleate from the liquid then:

$$I(t) = I_\alpha(t) + I_m(t), \tag{8}$$

$$F(t) = F_\alpha(t) \cdot F_m(t), \tag{9}$$

and

$$N(t) = N_o\, F_\alpha\, F_m \tag{10}$$

The rates of solidification of species α and m are then:

$$\frac{dN_\alpha}{dt} = \frac{v}{n_\alpha}\, I_\alpha\, N; \quad \frac{dN_m}{dt} = \frac{v}{n_m}\, I_m\, N \tag{11}$$

Substituting the value of F_α and F_m from equation 7 and combining equations 10 and 11 gives:

$$\frac{dN_\alpha}{dt} = N_o\, \frac{v}{n_\alpha}\, I_\alpha(t) \exp\left[-v \int_o^t \left[\frac{I_\alpha(z)}{n_\alpha} + \frac{I_m(z)}{n_m}\right] dz\right] \tag{12}$$

so that:

$$\frac{N_\alpha(t)}{N_o}\Big|_o^\infty = \frac{v}{n_\alpha}\int_o^\infty I_\alpha(t)\exp\left[-v\int_o^t\left[\frac{I_\alpha(z)}{n_\alpha}+\frac{I_m(z)}{n_m}\right]dz\right]dt \quad (13)$$

and

$$\frac{N_m(t)}{N_o}\Big|_o^\infty = \frac{v}{n_m}\int_o^\infty I_h(t)\exp\left[-v\int_o^t\left[\frac{I_\alpha(z)}{n_\alpha}+\frac{I_m(z)}{n_m}\right]dz\right]dt \quad (14)$$

Equations 13 and 14 give the respective fractions of the original liquid droplets appearing as species α and m. Therefore, the ratio of the metastable solid phase to the stable solid phase neglecting solid state transformations is:

$$R = \frac{N_m(t)\Big|_o^\infty}{N_\alpha(t)\Big|_o^\infty} \quad (15)$$

Quenching Rates of Liquids

Plummer[1] and the authors as shown later have observed that completely melted alumina particles show varying degrees of porosity. It is assumed that gases are entrapped in the liquid and cause bubble formation. If on being subjected rapidly to ambient conditions a molten spherical shell loses heat both by conduction and convection and steady state gradients are rapidly established then:

$$q = \frac{4\pi r^2 \Delta T}{\frac{r-r_o}{k\, r_{o/r}} + \frac{1}{h_s}} \quad (16)$$

where:

q = heat lost by the hollow sphere in cal. per sec.

r = outer radius of the sphere.

r_o = inner radius of the sphere.

k = the thermal conductivity of the liquid.

h_s = surface heat transfer coefficient.

ΔT = temperature gradient from the inner shell of the sphere to

to the ambient temperature.

The above equation is not applicable to solid spheres (i.e., $r_{o/r} = 0$.)

The cooling of the particle may be described by:

$$\frac{\text{Heat removed}}{\text{sec °C}} (T-T_o) = - m C_p \frac{dT}{dt} \tag{17}$$

where:

m = mass of the sphere.

C_p = specific heat of the liquid.

T = mean temperature of the particle.

T_o = ambient temperature.

Combining equations 16 and 17 gives:

$$\frac{4}{3} \pi r^3 \frac{\rho_a}{\rho_t} C_p \frac{dT}{dt} = - \frac{4 \pi r^2 (T-T_o)}{\frac{r-r_o}{k r_{o/r}} + \frac{1}{h_s}} \tag{18}$$

where:

ρ_a = apparent density of the liquid sphere.

ρ_t = true density of the liquid sphere.

therefore:

$$\frac{dT}{T-T_o} = \frac{-3 \rho_t k \, dt}{C_p \rho_a r \left(\frac{r-r_o}{r_{o/r}} + \frac{k}{h_s} \right)} \tag{19}$$

In the case where $\frac{k}{h_s} \ll \frac{r-r_o}{r_{o/r}}$ and T_m is the initial temperature of the particle, then:

$$\ln \frac{(T-T_o)}{(T_m-T_o)} = \frac{-3 \rho_t k t}{C_p \rho_a r^2 \left(\frac{1 - r_{o/r}}{r_{o/r}} \right)} = -C f(\rho_a, r) t \tag{20}$$

where:

$$\frac{1-r_{o/r}}{r_{o/r}} = \left[\frac{1}{\left(1-\frac{\rho_a}{\rho_t}\right)^{1/3}} - 1\right] \tag{21}$$

for small values of t:

$$T-T_o \approx \left(T_m-T_o\right)(1-\lambda t) = C_2\,(1-\lambda t) \tag{22}$$

where:

$$C_2 = T_m - T_o$$

$$\lambda = C\, f\left(\rho_a, r\right)$$

By combining 22, 13, 14, and 15 and changing variables such that $x = \lambda C_2 z$ and $y = \lambda C_2 t$ in equation 13 and 14 we obtain:

$$R = \frac{n_\alpha}{n_m} \frac{\int_o^\infty I_m(y) \exp\left[-\frac{v}{\lambda C_2}\int_o^y \left(\frac{I_\alpha(x)}{n_\alpha} + \frac{I_m(x)}{n_m}\right) dx\right] dy}{\int_o^\infty I_\alpha(y) \exp\left[-\frac{v}{\lambda C_2}\int_o^y \left(\frac{I_\alpha(x)}{n_\alpha} + \frac{I_m(x)}{n_m}\right) dx\right] dy} \tag{23}$$

This equation gives R, the ratio of metastable to stable phase, as a function of $\frac{v}{\lambda C_2}$. Plotting ln R vs. λ should give a continuous function provided all the crystalline particles feed into a arc plasma torch are completely melted.

EXPERIMENTAL PROCEDURE

Feed Material, Plasma Arc Melting, and Particle Recovery

Commercial sapphire boules were crushed and separated by sieving and air elutriation into narrow particle size ranges. These were subsequently spheroidized in the plasma jet using an argon-10 volume percent hydrogen plasma gas and an argon carrier gas. High speed motion pictures of the emergent particles indicated their velocity to be of the order 500 feet per second. The plasma flame extended approximately 4 inches from the torch tip giving a residence time of the particle in the hot zone of about one millisecond. The emergent particles entered a water cooled stainless steel collection chamber (Figure 3a).

The quenching rate was considerably reduced in one set of experiments by allowing the emergent particles to enter a heated tube furnace (Figure 3b).

In all runs a fraction of the particles were not spheroidized. The nonspherical particles above 37 microns were removed from the batch by allowing the sperical particles to roll down a vibrated inclined polished metal surface. For particle sizes below 37 microns the fraction of unspheroidized particles was estimated by microscopic examination and assumed to be all α alumina.

The spheroidized material from any particular size feed always had a considerably wider size distribution than the feed. This distribution could arise from both gas entrappment and from the particle shape encountered in separating the feed material. Considering the inital feed particle size and the final spheroidized particle size and apparent density, it was estimated that agglomeration of the feed particles was negligible.

The spheroidized material after separation of the unmelted angular particles was divided into size fractions by screening and were further divided on the basis of their apparent density by air elutriation. Therefore, from any one size fraction feed, a series of fractions was obtained varying in their size and apparent density. The value of the apparent density was subsequently determined by a pycnometer.

X-ray Diffraction Analysis

X-ray powder diffraction was used for both phase identification and semi-quantitative analysis of the volume fraction of phases present. The amount of all metastable phases was collectively reported in the analysis. The total area under six x-ray diffraction lines for the metastable phases was compared to the area under selected alpha alumina lines depending on the alpha content of the sample (Table I).

Table I

X-ray Diffraction Lines Used in Semiquantitative Analysis of Phases Present in Quenched Alumina Spheres

Alpha Phase		Metastable Phases		
Greater than 90 volume percent, "d" spacing in Å	Less than 90 volume percent, "d" spacing in Å	Phase	"d" spacing in Å	
		δ	2.59	
1.099	2.552	δ	2.46	
1.078	2.089	δ	2.277	Combined area
0.998	1.601	γ	2.28	
		δ	1.989	Combined area
		γ	1.980	

Table II

Analysis of Spheroidized Material from a Feed Size Range of 53 to 61 microns

Size range in microns	Apparent density ρ_a (gms/cm^3)	ln R	Size range in microns	Apparent density ρ_a (gms/cm^3)	ln R
44-53	2.35	1.00	61-74	3.16	-0.92
53-61	2.04	1.01	74-88	1.26	1.94
"	3.01	-0.25	"	1.78	1.02
"	3.72	-2.66	"	2.74	-0.76
61-74	1.62	1.61	88-104	1.08	1.34
"	2.24	0.74			

Microscopic Analysis

Direct microscopic observation of the spheroidized material was made by mixing the spheres with powdered glass of the same thermal expansion coefficient and hot pressing (below 650 °C) the mixture in vacuum to obtain a dense composite. This composite was then polished and the alumina particles etched with ortho-phosphoric acid. For observation of the surface, a thin gold layer was vapor plated on the surface prior to examination with the metallographic microscope. This gold layer decreased the internal reflections. Thin sections were prepared of selected samples to obtain the optical properties of the phases showing different etching characteristics under metallographic examination.

Other Analysis

Differential thermal analysis was made on spheroidized material which by x-ray examination was found to be above eighty percent of the metastable phases. This same material was heated to various temperatures for extended times and the weight loss and relative amounts of the phases present determined. Infrared analysis between two and fifteen microns was made by the potassium bromide pelletizing technique. Infrared absorption curves were obtained for the feed material, spheroidized material containing large amounts of the metastable phases and gamma alumina formed by dehydrating aluminum hydroxide.

RESULTS AND DISCUSSION

Identification of Phases

The plasma torch was operated under constant conditions of plasma current, primary and carrier gas flow rate, and cooling water flow, and the geometry of the particle collection chamber was maintained constant. Decreasing the size of the feed particles gave increased amounts of metastable phases as indicated by both x-ray and microscopic analysis.

Microscopic examination by metallographic techniques indicated that many particles were hollow spheres as shown in Figure 4a. The etching characteristics of individual spheres were found to differ, with some relatively unattacked by the ortho-phosphoric acid, and others severely attacked (Figure 4b). Except in a few isolated cases, the spheres obtained showed only one type of acid attack indicating only one crystalline phase present. Thin sections of the hollow spheres under the petrographic microscopy with crossed nichols showed that those particles unattacked by the acid gave extinctions identical to alpha alumina while those exhibiting etched surfaces, had complete extinction.

X-ray diffraction of material fed through the plasma jet indicated that phases other than alpha alumina were present and that the amount of other phases agreed with the microscopic examination. Spheres of small size or low density gave very low intensity alpha lines, high intensity lines agreeing with gamma lines obtained by Stumpf[4] and other lines of decreased intensity that were similar to the delta lines identified by Rooksby[16]. The last had some exceptions that are noted below. Increasing the sphere size or density gave increasing intensity ratio of both, alpha to the combined metastable phase lines, as well as an increased ratio of delta to gamma lines. However, the 1.950, 1.989, and 2.277Å lines given by Rooksby as comparatively strong delta lines, were either negligible or absent in the phases identified as delta. Therefore, the metastable phases formed in this investigation are tentatively identified as gamma and delta alumina. Others[1, 2, 3] have identified delta and gamma alumina as being present in quenched samples. Theta alumina has also been reported.[1]

Differential thermal analysis of samples containing over 80 percent of metastable phases gave one exothermic peak starting at 1130 °C the reaction being completed by 1200 °C. This agrees with the reported transformation

temperature range for the converstion of metastable phases formed by dehydration of hydroxides to alpha alumina [4] in the absence of stabilizing impurities. Heating samples with large amounts of metastable phases for 18 hours at 800 °C did not change the x-ray diffraction patterns or indicate any loss in weight. Heating to 1200 °C showed less than 0.005 percent loss in weight with complete conversion to alpha alumina.

Infrared absorption spectra of a sample containing a large fraction of metastable phases (primarly gamma) gave essentially the same spectra as gamma alumina prepared by heating alpha monohydrate to 825 °C for two hours except that a strong OH absorption band at 2.9 microns present in the second case was missing in the former.

The metastable phases found in this investigation differ from those found by Plummer. [1] Plummer obtained primarly delta and theta in quenching from an oxygen-hydrogen flame, whereas severe quenching was obtained in this study by use of the plasma jet.

Heat Transfer

All particles of one size when fed into the plasma torch should heat at approximately the same rate. However, when melted and injected into a cold gas, their cooling rate will depend on their diameter, apparent density, etc. as given in equation 20. Radiative heat transfer during cooling of the liquid particles was discounted following the arguments of Gardon [15] who showed that for optically translucent materials of small thickness, the total emissivity is directly proportional to thickness and would, in this case where thicknesses are less than 10^{-2} cm., be negligibly small.

One modified collection chamber geometry was attempted as shown in Figure 3b. The tube into which the particles emerged after being melted in the plasma was heated by the torch gases prior to starting the particle feed. Spheres from this experiment when compared to the spheres obtained under

identical conditions except for the heated tube showed a decreased amount of metastable phases. This is in agreement with the hypothesis advanced previously that the greater the quenching rate of a liquid droplet the greater the amount of metastable phases present in the solid.

Analysis of Fractionated Spheres

Feed particles in size fractions from 9-13 microns to 88-104 microns were spheroidized and the hollow sphere fraction separated. The yield of hollow spheres obtained was above fifty percent of the feed. The product of each run was separated into size fractions by sieving and further classified into apparent density fractions by air elutriation. The ratio of the metastable phases to alpha alumina was then determined for each fraction. Typical results are shown in Table II.

The ratio of the volume of metastable phases to the volume of alpha alumina vs. the apparent density for all runs was plotted and is shown in Figure 5. The points corresponding to a given range of sphere diameters fall on a continuous band. Because of the width of both the size range and apparent density range, the trend of the data points rather than specific relations are observed. As the size of spheres of one apparent density decreases, the ratio of metastable to stable phase increases. This is in agreement with equation 23.

Figure 6, where the ratio of metastable to stable phases is plotted vs. the function $\rho_a r^2 \left[\frac{1}{\left(1 - \frac{\rho_a}{\rho_t}\right)^{1/3}} - 1 \right]$, shows a continuous band of points as would be expected from equation 23. The plot so obtained also indicates that the ratio $\frac{n_m}{n_\alpha}$ remains constant and that $\frac{v}{n}$ for both metastable and stable phases remains constant for the range of experimental conditions. Microscopic examination of spheres such as shown in Figure 4b indicated that the alpha alumina particles are made up of one or a few grains. Grain boundaries were

evident in many hollow alumina spheres. No determination of the number of grains present in the metastable spheres could be made due to the severe uniform attack of the surface by the acid etch.

CONCLUSIONS

The general observations of Plummer[1] that; (a) the smaller the feed particles of alpha alumina the greather the transformation to metastable phases on rapid quenching of liquid droplets, (b) individual spheres obtained from quenched molten alumina are of a single phase, (c) moderate quenching conditions from the liquid state accentuate the formation of delta alumina, (d) the heat conductivity of the liquid probably determines the heat transfer in quenching alumina, and (e) the larger the spherical particle from quenching molten alumina the lower its apparent density agree with the findings in this investigation.

His objections to considering the cooling rate of molten alumina droplets as the sole criterion for transformation to metastable crystalline phases are based mainly on; (a) his observation of a break in the transformation ratio-radius curve in the neighborhood of 15 to 35 microns, and (b) the inability to find mixtures of metastable and alpha alumina in individual particles which he expected, if the ratio of phases present were to be a continuous function of cooling rate.

In this investigation a continuous variation of the ratio of the metastable to stable phases vs. the quenching rate was found as proposed in the hypothesized mechanism. Also, if nucleation is followed by rapid growth as proposed in the hypothesis then individual particles should and did show only one crystalline solid phase after quenching a liquid droplet. Therefore, the two primary objections made by Plummer to the quenching rate being the criterion of primary importance in the solidification mechanism of molten alumina can be countered by the proposed hypothesis on the nucleation kinetics and its

relationship to quenching rates.

The absence of weight loss on heating and the observed infrared absorption spectra of the metastable phases rule out OH stabilization that has been porposed as a mechanism for the formation of similar metastable phases formed by decomposition of hydrates or other aluminum salts. The purity of the feed material minimized the presence of stabilizing impurities. Plummer's observation of the independence of the ratio of metastable to stable phases on the feed material (gamma or alpha alumina) and the results obtained in this investigation when the particle collection chamber geormetry was changed keeping heating conditions unaltered suggest that an "associated " liquid structure does not influence the nucleation of a crystalline phase from molten alumina under severe quenching conditions.

The evidence of a continuous variation of the ratio of metastable crystalline phases with respect to the quenching parameter [$f(\rho_a, r)$] for molten alumina droplets lends reasonable support to the hypothesis that the nucelation rate curves determine the crystalline phase obtained.

ACKNOWLEDGMENTS

The authors gratefully acknowledge the helpful discussions with D. R. Olander and J. A. Pask.

This work was done under the auspices of the U.S. Atomic Energy Commission.

LITERATURE REFERENCES

1. M. Plummer, J. Appl. Chem. (London) 8. (1958) 35-44.
2. H. Meyer, Ber. Deut. Keram. Ges., 39 [2] (1962) 115-122.
3. N. N. Ault, J. Am. Ceram. Soc., 40 (1957) 69-74.
4. J. W. Newsome, H. W. Heiser, A. S. Russel, and H. C. Stumpf, Alcoa Research Laboratories Technical Paper No. 10 (second revision) Alcoa, Pittsburgh, Pa., U.S.A. (1960) 88 pp.
5. M. Hoch and H. L. Johnston, J. Am. Cehm. Soc. 76 (1945) 2560-1.
6. Von K. Torkar and H. Krischner, Ber. Deut. Keram. Ges., 39 [2] (1962) 131-35.
7. A. M. Kalinina, Zhur. Neorg. Khim. 4 (1959) 1260-9, Chem. Abst. 54 [11] (1960) 10481b.
8. A. L. Kozlovskii and K. S. Shlyakova, Trudy Vsesoyuz. Nauch-Issledovatel., Inst. Autogen. Obrabotki Metal. 6 (1960) 136-9, Chem Abstr. 55 [17] (1961) 16062f.
9. J. Frenkel, "Kinetic Theory of Liquids," Dover Plublications, Inc., New York (1955) (a) p. 387, (b) p. 394, eq. (24).
10. W. J. Dunning, "Chemistry of the Solid State," W. E. Garner, Ed., Butterworths Scientific Publications, London (1955) p. 169, eq. (50).
11. J. D. Mackenzie, "Adv. in Inorg. Chem. and Radio Chem.," H. J. Emeleus and A. G. Sharpe, Ed., 4 (1962) 293-318.
12. W. L. Bade and R. R. John, J. Am. Roc. Soc., 1 (1961) 4-17.
13. W. B. Hillig, "Symposium on Nucleation and Crystallisation in Glasses and Melts," Am. Ceram. Soc., (1962) 77-89.
14. J. A. Cahill and A. D. Krishbaum, J. Inorg. and Nucl. Chem. 14 (1960) 283-87.
15. R. Gardon, J. Am. Ceram Soc., 39 [8] (1956) 278-287.
16. H. P. Rooksby, J. Appl. Chem. (London), 8 (1958) 44-49.

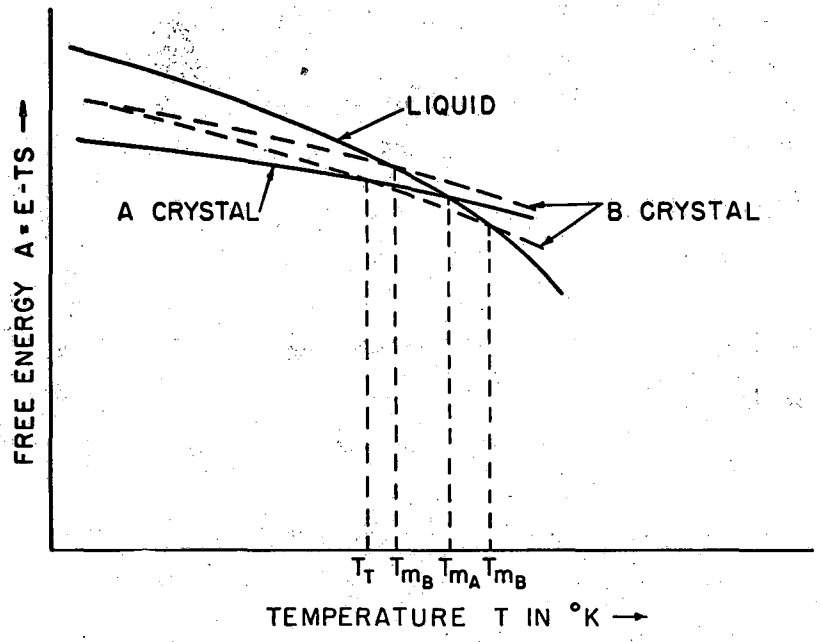

FIG. I. DIAGRAMMATIC PLOT OF FREE ENERGY VERSUS TEMPERATURE.

MU-33499

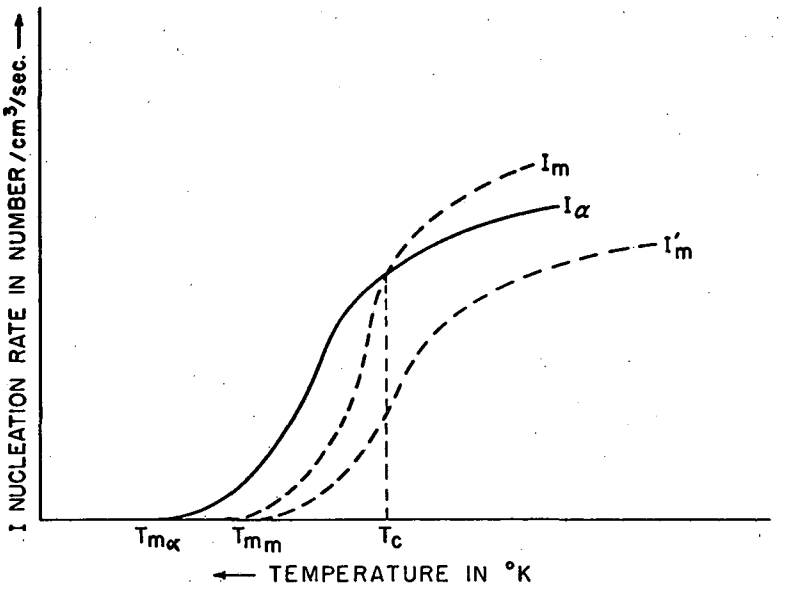

FIG. 2. DIAGRAMMATIC PLOT OF NUCLEATION RATE VERSUS TEMPERATURE.

MU-33500

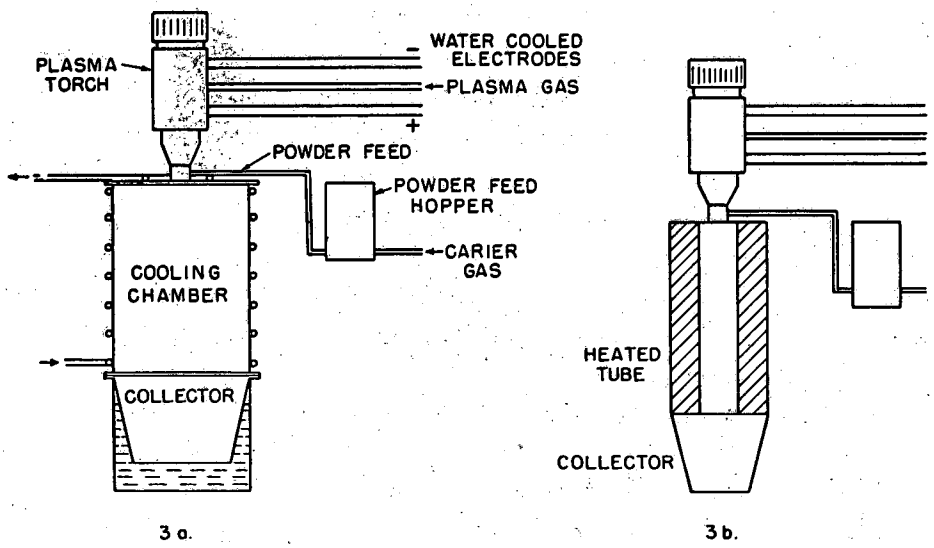

FIG. 3. DIAGRAMMATIC SKETCH OF PLASMA TORCH WITH QUENCHING AND COLLECTION CHAMBER.

MU-33501

Figure 4. (a) Spheroidized alumina particles mounted in a glass matrix. The alumina spheres are the hollow particles; the solid appearing particles are glass surfaces attacked by the etchant. (b) Higher magnification of 4a showing the difference in etchant attack on individual alumina spheres.

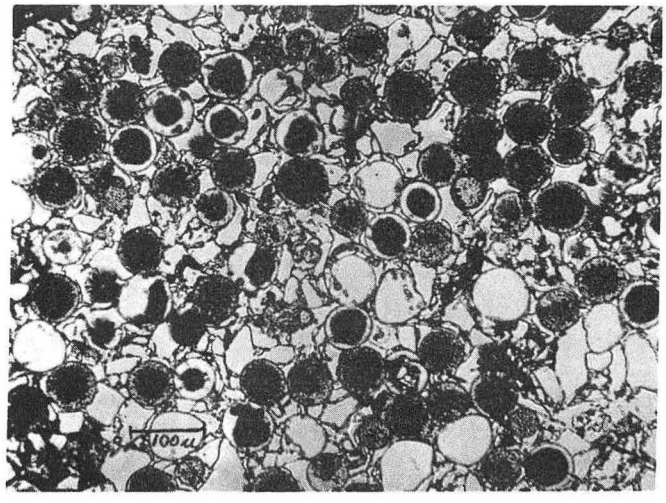

(a)

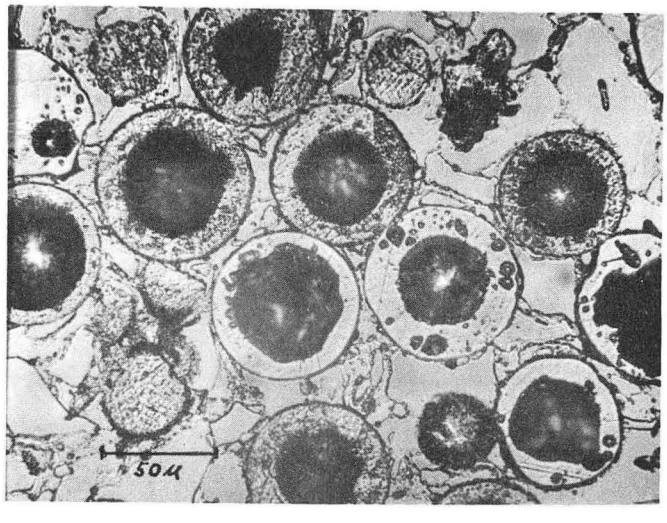

(b)

ZN-4150

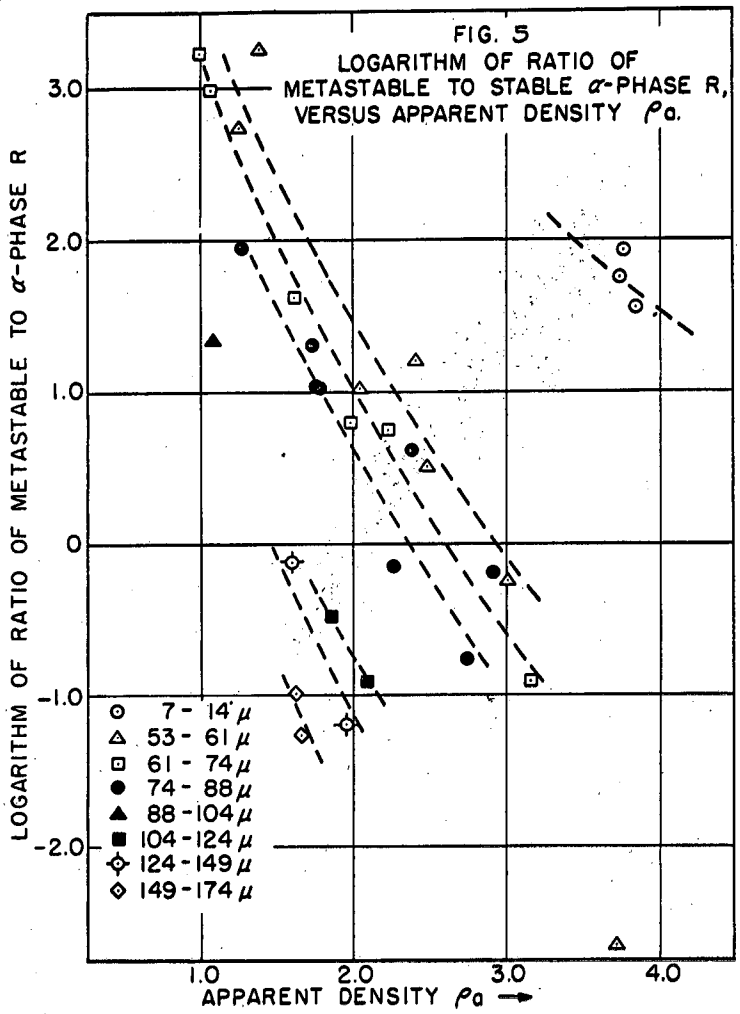
FIG. 5
LOGARITHM OF RATIO OF METASTABLE TO STABLE α-PHASE R, VERSUS APPARENT DENSITY ρa.
LOGARITHM OF RATIO OF METASTABLE TO α-PHASE R
3.0
2.0
1.0
0
-1.0
-2.0
1.0
2.0
3.0
4.0
APPARENT DENSITY ρa →
7 - 14 μ
53 - 61 μ
61 - 74 μ
74 - 88 μ
88 - 104 μ
104 - 124 μ
124 - 149 μ
149 - 174 μ
MU-33502

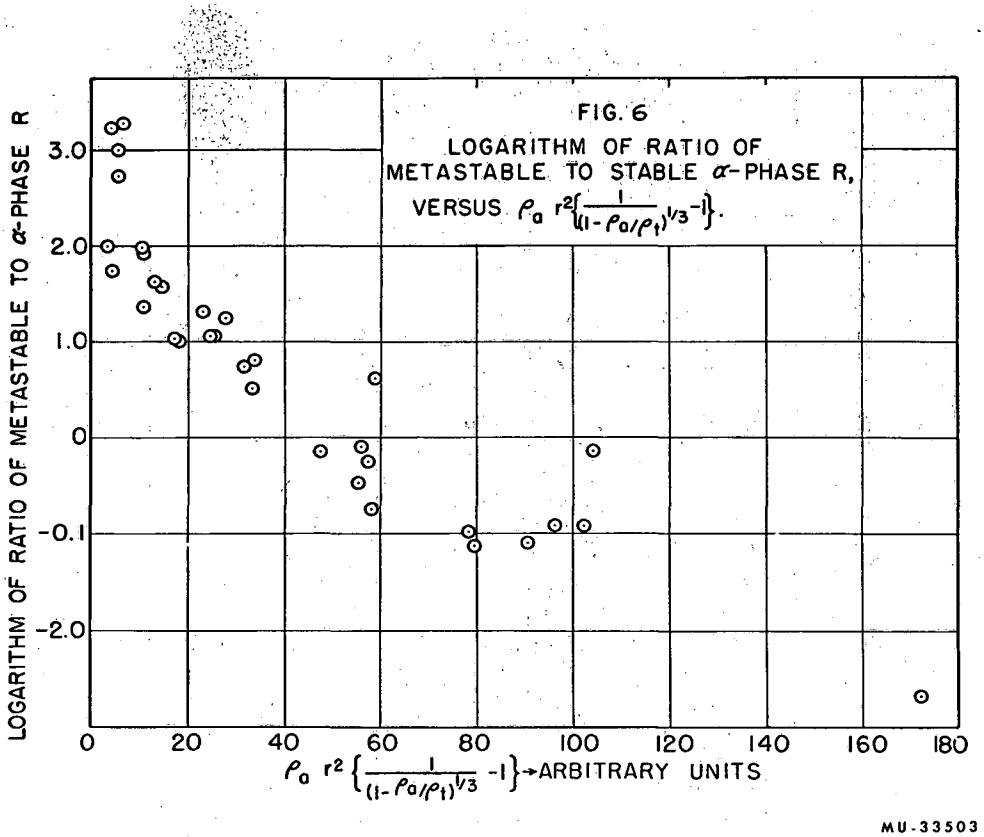
FIG. 6
LOGARITHM OF RATIO OF METASTABLE TO STABLE α-PHASE R, VERSUS $\rho_a r^2\left\{\frac{1}{(1-\rho_a/\rho_t)^{1/3}}-1\right\}$.
LOGARITHM OF RATIO OF METASTABLE TO α-PHASE R
3.0
2.0
1.0
0
-0.1
-2.0
0
20
40
60
80
100
120
140
160
180
$\rho_a r^2\left\{\frac{1}{(1-\rho_a/\rho_t)^{1/3}}-1\right\}$ → ARBITRARY UNITS
MU-33503